Plant Methods

METHODOLOGY

Open Access

Combining Fourier-transform infrared spectroscopy and multivariate analysis for chemotyping of cell wall composition in Mungbean (*Vigna radiata* (L.) Wizcek)

Shouvik Das[1*], Vikrant Bhati[1], Bhagwat Prasad Dewangan[1], Apurva Gangal[1], Gyan Prakash Mishra[2], Harsh Kumar Dikshit[2] and Prashant Anupama Mohan Pawar[1*]

Abstract

Background Dissection of complex plant cell wall structures demands a sensitive and quantitative method. FTIR is used regularly as a screening method to identify specific linkages in cell walls. However, quantification and assigning spectral bands to particular cell wall components is still a major challenge, specifically in crop species. In this study, we addressed these challenges using ATR-FTIR spectroscopy as it is a high throughput, cost-effective and non-destructive approach to understand the plant cell wall composition. This method was validated by analysing different varieties of mungbean which is one of the most important legume crops grown widely in Asia.

Results Using standards and extraction of a specific component of cell wall components, we assigned 1050–1060 cm^{-1} and 1390–1420 cm^{-1} wavenumbers that can be widely used to quantify cellulose and lignin, respectively, in Arabidopsis, *Populus*, rice and mungbean. Also, using KBr as a diluent, we established a method that can relatively quantify the cellulose and lignin composition among different tissue types of the above species. We further used this method to quantify cellulose and lignin in field-grown mungbean genotypes. The ATR-FTIR-based study revealed the cellulose content variation ranges from 27.9% to 52.3%, and the lignin content variation ranges from 13.7% to 31.6% in mungbean genotypes.

Conclusion Multivariate analysis of FT-IR data revealed differences in total cell wall (600–2000 cm^{-1}), cellulose (1000–1100 cm^{-1}) and lignin (1390–1420 cm^{-1}) among leaf and stem of four plant species. Overall, our data suggested that ATR-FTIR can be used for the relative quantification of lignin and cellulose in different plant species. This method was successfully applied for rapid screening of cell wall composition in mungbean stem, and similarly, it can be used for screening other crops or tree species.

Keywords Plant cell wall, Mungbean, Cellulose, Lignin, FT-IR

*Correspondence:
Shouvik Das
shouvik.das@rcb.res.in
Prashant Anupama Mohan Pawar
prashant.pawar@rcb.res.in
Full list of author information is available at the end of the article

Introduction

The plant cell wall is a complex polymeric network structure that is mainly composed of cellulose, hemicellulose, lignin and pectin. The diversity in plant cell shapes and sizes is determined by several factors, including distinct physicochemical properties of the cell wall which play pivotal roles such as morphogenesis, providing mechanical support, transporting nutrients and water, and defending against different environmental stresses [1–5]. The plants consist of several types of cells [2, 6] which have distinct and dynamic cell wall compositions and organization. The structural diversity of cells is due to the complex chemical and structural heterogeneity of plant cell wall. Also, in the last couple of decades, the focus has been shifted to understanding the genetic regulation of the cell walls and these efforts have identified many biosynthetic, modifying enzymes and transcription factors [2, 7]. These studies are mainly related to selected species like Arabidopsis, *Populus*, rice, Brachypodium, and Eucalyptus. More focus is now needed to understand the regulation in plant cell walls of different economically important crop species to identify the genes involved in cell wall biosynthesis by exploiting natural variation in species followed by quantitative trait loci identification and validation using genome editing tools. To attain this, it is necessary to understand the qualitative and quantitative composition of the plant cell wall. Many wet chemistry-based strategies are available for cellulose and lignin quantification [8, 9]. Matrix polysaccharide sugars are quantified by derivatization and detection with GC–MS [10] but these methods are laborious and time-consuming. Biophysical methods such as pyrolysis gas chromatography-mass spectroscopy, Raman spectroscopy, and Fourier transformation infrared spectroscopy (FTIR) can be also used for studying the cell wall composition [11, 12]. The main advantage of the pyrolysis-based approach is that it does not require the pre-treatment of cell wall material. It is rapid and highly reproducible which requires less sample weight; however, it can relatively quantify only total carbohydrate content and lignin composition [13]. The Raman and FTIR spectroscopy are also non-destructive approaches to studying plant cell wall properties [14]. The limitation of both methods is that molecular vibrations of all molecules result in many overlapping bands. Thus, it is also challenging to understand and interpret the acquired spectra. Therefore, it is highly imperative to implicate a rapid and accurate method for plant cell wall analysis. Attenuated total reflectance (ATR)-FTIR has been used for fast cell wall characterization [15]. The ATR-FTIR spectroscopy is widely applicable for the chemical analysis of biological materials. It is relatively high throughput, inexpensive, requires simple sample preparation and less sample size as compared to wet chemistry-based or chromatographic methods. In ATR- FTIR, a wide range of spectra can be generated for either powders, liquids, or pastes with a minimum of sample preparation, reducing the analysis time [16–20]. Moreover, the spectral data can be exploited using multivariate statistical techniques for quantitative applications based on the relationship between spectral and reference data obtained by conventional methods. This data can be used to build predictive models and qualitative applications to infer diversity and classify samples according to their spectral characteristics. In ATR-FTIR, the absorption spectra are generated because of molecular vibration which leads to a change in dipole moment. The absorption frequency depends on the functional group, which varies between different cell wall molecules [21]. Cell wall composition may be determined by predicted equations based on near-infrared absorbance spectra of ground plant materials. This technique has been successfully used to understand the cell wall composition in Arabidopsis [22, 23], forage crops [24–28], rice [29, 30] and *Populus* [31, 32]. The quality of the spectra depends on the selection of sampling methods and the total internal reflectance of the ATR-FTIR beam. In this technique, the accuracy of the measurement depends on the direct contact between the sample and the ATR crystal surface [33]. Therefore, the solid or powdered sample, must be clamped using pressure gauges onto the crystal surface that can be either semiliquid or liquid form. The Beer-Lambert law and multivariate chemometric analysis can be performed for fast and accurate quantification using ATR-FTIR. The law states that the path length and concentration of given sample are directly proportional to the absorbance of the light which is represented by this equation—$A = \log_{10}(Io/I) = \epsilon lc$. In this equation, *A*, *Io*, *I*, ε, l and c represent the absorbance of the sample, initial light intensity; light intensity; molar extinction coefficient; distance covered by the light through the solution; and the concentration of the absorbing sample respectively [34, 35].

The qualitative and quantitative accuracy of analysis in ATR-FTIR also depends on the homogenization of the sample. However, the homogenization of plant cell wall material is difficult and untreated native cell wall materials do not dissolve in organic solvents. Therefore, the powdered cell wall material can be quantified using two classical methods, the KBr pellet method and the Nujol method [36]. The KBr pellet is the most common alkali halide which becomes stiffy when subjected to pressure and forms a transparent sheet that can be used to measure the infrared spectrum in the 600 to 4000 cm^{-1} wavenumber regions. Generally, the sample is well mixed and pulverized with KBr, which can stabilize the pellet and be subjected to ATR-FTIR.

Using the KBr-based pellet method, we have established a non-destructive high-throughput phenotyping method to analyse cell wall composition using ATR-FTIR spectroscopy. This method can be used for qualitative and quantitative analysis of solid cell wall material that is not dissolved in organic solvent. The cellulose and lignin standards were prepared in KBr and standard curve was used for quantification of the above components in different species. The cell wall composition was further cross-validated using wet-chemistry-based method in different plant and tissue types. Besides, cellulose and lignin content were measured using a developed ATR-FTIR-based approach and validated chemically among a set of 48 genotypes of mungbean which suggested that this method can be used for quantitative analysis in a high throughput manner.

Materials and methods

Plant growing, tissue collection and processing

In this study, the leaf and stem of crop species like rice (*Oryza sativa* subsp. *Indica*), *Populus* (*Populus trichocarpa* L.), mungbean (*Vigna radiata* (L.) *R. Wilczek*) and Arabidopsis (*Arabidopsis thaliana)* have been analyzed. Arabidopsis was grown under 16 h light/8 h dark cycle conditions at 22 °C. Rice was grown under 14 h light/10 h dark at 26 °C with 85% relative humidity. Mungbean was grown under 16 h light/8 h dark at 32 °C. Mature leaf tissues of rice, mungbean and Arabidopsis were harvested from fully grown healthy plants grown in a well-managed field at Regional Centre for Biotechnology, Faridabad (Latitude: 28°4052° N; Longitude: 77.2532° E). The *Populus* stem and leaf tissues were collected from Forest Research Institute (FRI), Dehradun, India (Latitude 30.343769° N; Longitude is 77.999559° E). The fresh leaf and stem tissues were harvested and ground into fine powder using QIAGEN Tissue Lyser (TissueLyser III, Cat. No. 9003240, Germany).

Preparation of alcohol insoluble residues (AIR) to isolate cell wall material

100 mg of crude powder was incubated with 5 mL ethanol (80%) containing 4.0 mM HEPES buffer (pH 7.5) at 70 °C for 30 min, cooled on ice, and centrifuged (10,000 rpm; 15 min). The pellet was washed with 5 ml of 70% ethanol, and further treated with 5 ml chloroform: methanol (1:1). The remaining pellet was washed with 5 mL of acetone, pellet obtained after centrifugation was dried in the desiccator and this AIR sample was used for further analysis [37].

ATR- FTIR spectroscopy

The AIR, along with KBr, was used to prepare the FT-IR standards. The ATR-FTIR spectra of the powdered sample was measured, and the mixture was subjected to a Tensor FTIR spectrometer (Bruker Optics) equipped with a single-reflectance horizontal ATR cell (ZnSe Optical Crystal, Bruker Optics). Between scanning range from 600 to 4000 cm^{-1} with a resolution of 4 cm^{-1}. A pressure applicator with a torque knob ensured that the same pressure was applied for all measurements. For each sample, 16 scans were acquired, averaged with a background scanning and correction of 15–20 min regular intervals. The standard deviations of spectra of the subsamples were obtained by the OPUS 5.5 software (Bruker Optics, http://www.brukeroptics.com/). The standard deviations of the different biological samples were used to create an overall standard deviation using the multi-evaluation tool in the OPUS software.

Estimation of cellulose content using the Updegraff method

2 mg of AIR was incubated at 100 °C for 30 min in Updegraff reagent, and the pellet obtained after centrifugation was washed with water and acetone. The dried pellet was treated with concentrated sulphuric acid and glucose was quantified by anthrone assay [38].

Acetyl bromide soluble lignin content (ABSL)

2 mg of AIR was incubated in freshly prepared 25% acetyl bromide (prepared in acetic acid) in screw cap tubes at 50 °C for 2 h. The solubilized lignin was mixed with 400 µl of 2 M sodium hydroxide, 70 µl of 0.5 M hydroxylamine hydrochloride and diluted with 1430 µl of acetic acid. 85 µl of this reaction mixture was mixed with 85 µl of acetic acid into a Corning® UV-transparent microplates (Corning, CLS3635, USA) and absorbance was taken at 280 nm using spectrophotometer [39].

Histochemical staining

Histochemical staining was performed by following Mitra and Loqué (2014) [40]. Briefly, 7–8 week old Arabidopsis plant, 3–4 week old mungbean plant and 8–9 week old rice plant were grown in controlled condition. For phloroglucinol staining, 10 µm stem sections were stained with 2% phloroglucinol in 95% ethanol and concentrated HCl (v/v, 2:1) for 5 min. For toluidine blue O staining, the 10 µm stem sections were stained with 0.02% toluidine blue solution. All the samples were observed under a light microscope and photographed using a NIKON Y-TV55 digital camera.

Total sugar estimation

The AIR samples were mixed in deionized water at a concentration of 0.5 mg/mL 100 µl of this AIR suspension sample was mixed with equal volume of 5% (v/v) phenol. Then, 500 µl of concentrated sulfuric acid was added

and incubated for 20 min. 250 µl of each reaction mixture was transferred into a Costar 3598 ELISA plate. The colour development in the reactions was measured using an ELISA plate reader by reading the OD at 490 nm. A standard curve of glucose was used to calculate glucose content in AIR sample.

Extraction of lignin

The AIR sample was treated with 1 mL of 4 M KOH containing 1.0% (w/v) sodium borohydride and incubated for 24 h with constant shaking [41]. After centrifugation, the pellet was washed with water. The dried pellet was treated with CTec2 enzyme blend (SAE0020, Sigma-Aldrich, Country) at 45 °C for 24 h to remove cellulose and the pellet mainly containing lignin was dried and used for FT-IR analysis as a standard.

Results

ATR-FTIR analysis revealed 1050–1060 cm^{-1} and 1390–1420 cm^{-1} wavenumber regions for cellulose and lignin analysis respectively

In this study, leaf and stem tissues from *Populus*, rice, mungbean and Arabidopsis were used for cell wall compositional analysis using ATR-FTIR. In ATR-FTIR, the infrared spectrum from the sample is generated due to the superposition of light absorbance by functional groups of cell wall polymer (chemical information) and light scatter (physical information). ATR-FTIR spectra can be categorized into different regions, including the X–H stretching region (4000–2500 cm^{-1}), the triple-bond region (2500–2000 cm^{-1}), the double-bond region (2000–1500 cm^{-1}) and the fingerprint region (1500–600 cm^{-1}) [42, 43]. The spectral region 600–2000 cm^{-1} was used to analyze linkages by determining functional groups which can correspond to specific cell wall components [44–46].

The spectral data was obtained on the alcohol extracted fraction (AIR) of different species which led to the specific absorption characteristics because of distinct composition (Fig. 1a, b). The distinct peaks are commonly used to identify a particular functional group of a specific cell wall component [38]. The spectra exhibited high absorbance at specific wavenumbers characteristic of cell-wall polysaccharides, which resulted in a peak that was assigned to a particular functional group of a specific cell wall polysaccharide. In this study, different absorbance patterns or peak characteristics have been observed for different samples. According to previous studies, cellulose peaks were assigned to 1060–1072 cm^{-1} wave number for which (CO), (CC) and (OCH) ring in Arabidopsis and *Populus* [44, 47]. For aspen and acetobacter 1099–1115 cm^{-1} wavenumber was assigned to O–H, (CO) and (CC) ring of cellulose [46, 48]. Therefore, based on these reports and cellulose standards, we selected the range 1050–1060 cm^{-1} wavenumber for further analysis. Previously, lignin peaks were detected in different ranges of wavenumber. In Arabidopsis, aspen, barley and bamboo region 1502–1520 cm^{-1} wavenumber was used to detect aromatic C=C stretch of lignin [47, 49–52]. In another study, 1456–1465 cm^{-1} wavenumber was reported for the detection of CH_3 asymmetrical bending of lignin [53, 54]. In this study, a prominent peak, 1390–1420 cm^{-1} wavenumber was observed for C–H deformation aromatic skeletal, which was assigned to lignin. This peak was reported in flax, *Populus* and hardwood maple [53, 55] (Table 1). Based on these peaks or regions, we compared cell wall composition in different species and tissue types.

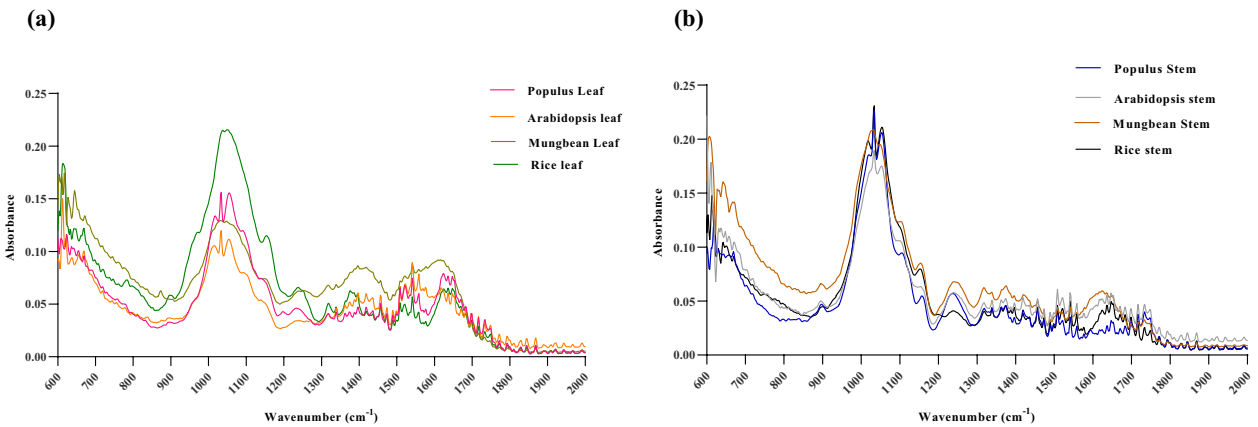

Fig. 1 Absorption spectral characteristics for different tissues of different plant samples using ATR-FTIR spectroscopy. The spectral mean was calculated from two biological replicates

Table 1 Specific characteristics of absorbance spectra for cellulose and lignin

Compound	Band position (cm^{-1})	Assignments	Sources and references
Cellulose	1050–1060	(CO), (CC), (OCH) ring	[67–69]
Lignin	1390–1420	C–H deformation Aromatic skeletal vibrations	[60, 70–72]

See Refs. [47, 55, 89–92]

The absorbance at different wavenumbers for different cell wall components clearly differentiated tissue of different plant samples (Fig. 1a, b). In the case of cellulose, within 1050–1060 cm^{-1} wavenumber higher absorbance was observed for *Populus* stem (0.20 ± 0.0025), rice stem (0.20 ± 0.0206), rice leaf (0.21 ± 0.0125) and mung stem (0.19 ± 0.0081). Leaf tissues reflected lower absorbance as compared to stem tissues. Among leaf tissues, *Populus* leaf (0.15 ± 0.0205) showed higher absorbance, followed by mungbean (0.12 ± 0.003) and Arabidopsis leaf (0.11 ± 0.002) for cellulose-specific peak. Interestingly, higher absorbance at the cellulosic region was observed for rice leaf. This may be due to the presence of higher hemicellulose (xylan) in rice leaf [56]. For lignin, within 1390–1420 cm^{-1} wavenumber, higher absorbance was observed for leaf samples than stem samples, which was further used to compare lignin content in different samples. Mungbean leaf lignin peak showed higher absorbance (0.085 ± 0.031) followed by rice leaf (0.05 ± 0.00165), Arabidopsis leaf (0.05 ± 0.00346), mungbean stem (0.048 ± 0.00145), *Populus* leaf (0.045 ± 0.00275), Arabidopsis stem (0.045 ± 0.00010), rice stem (0.041 ± 0.0015) and *Populus* stem (0.033 ± 0.00005). All these data correlated with existing knowledge of plant cell wall composition in different tissues or species, suggesting these wavenumber regions can be used for analysing cellulose (1050–1060 cm^{-1}) and lignin (1390–1420 cm^{-1}) across monocot, dicot and tree species.

Principal component analysis (PCA) based analysis of FT-IR data exhibited differences between stem and leaf tissue of different species

PCA has been successfully used to analyze FT-IR-generated spectral data to understand the differences and clustering in different groups [21, 57]. In this study, PCA was performed on raw data obtained from different spectral ranges and samples as explained earlier (Fig. 1). The most preferable spectral region for cell wall component analysis, i.e. 800–2000 cm^{-1} was used for PCA analysis. The score plot of the principal component was generated to identify differences in samples and model predictability. The scatter plot represented two principal components; PC1 and PC2, which together explain maximum variability in PCA within 800–2000 cm^{-1} range (Fig. 2a, Fig. S1a). The Q^2 and R^2 values were also checked for cross-validation. The Q^2 value represents the predictive ability of a model. It is an indicator to the degree of variation that is accounted for any dataset. The R^2 is a statistical measure that represents the goodness of fit of a regression model [58]. In this study, the Q^2 value was also significant, suggesting the PCA model was predictive (Fig. 2b). While comparing cell wall composition across different species and tissues, PC1 and PC2 showed 73% of the variability. The grouping effect was observed across both the axes. PC1 contributed to maximum variability (44.7%) as compared to PC2 (28.3%) (Fig. S1a, Fig. 2a). The grouping of the samples along the PC1 axis majorly represented stem samples of Arabidopsis, mungbean, *Populus* and rice. PC2 represented the leaf samples of Arabidopsis, mung bean and *Populus*. The PC1 grouping of rice leaves can be explained by the fact that rice leaves contain more cellulose and hemicellulose than other studied crops. This was well documented and validated through absorption spectral analysis, which was higher for rice leaf within 800–2000 cm^{-1} range [59, 60].

To specifically understand the variation in cellulose content in different species, PCA was used within the 1000–1050 cm^{-1} range (Fig. 2c, d, Fig. S1b). As expected, stems of *Populus*, Arabidopsis and mungbean clustered together, separated by PC2 component with 31.3% of the variability. These groups were separated from the leaf of mungbean, Arabidopsis and *Populus* and rice stem, which were clustered together. Rice leaf was grouped separately from the above tissue types. This data was further validated by K-mean clustering which indicated that cell wall components of the leaf and stem of monocot and dicot species have distinct structures (Fig. S2).

The PCA within region 1390–1420 cm^{-1} revealed lignin characteristics for different tissues and plant samples. PC1 and PC2 both contributed around 89% of the variation. PC1 exhibited highest variability of 57.8% (Fig. 2e, Fig. S1c). Also, a significant Q2 value suggested the predictive ability of the model (Fig. 2f). Rice stem, rice leaf and *Populus* stem clustered together and well separated from other tissues further confirming that the above wavenumber region is suitable to analyse lignin

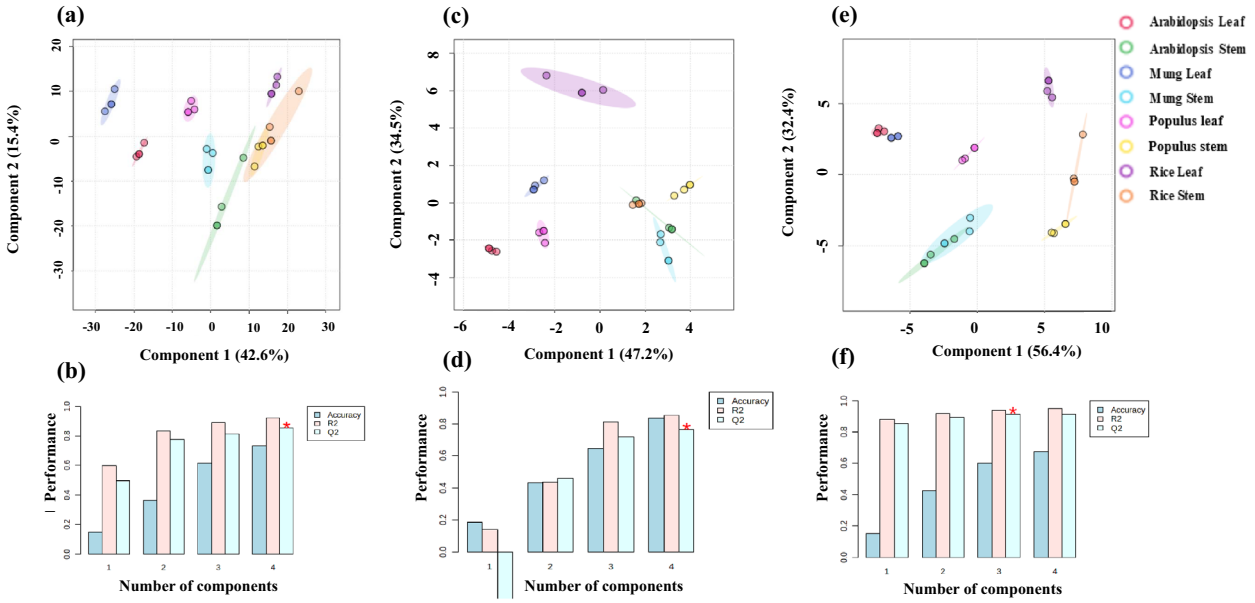

Fig. 2 Partial Least Squares Discriminant Analysis (PLS-DA) of absorption spectra and cross-validation using Q-square value within **a**, **b** 600–2000 cm^{-1} **c**, **d** 1000–1100 cm^{-1} and **e**, **f** 1390–1420 cm^{-1} wavenumber for total sugar, cellulose and lignin respectively in ATR-FTIR. These graphs were prepared using an online tool -https://www.metaboanalyst.ca/

content. Overall this data suggested that multivariate analysis using 800–2000 cm^{-1}, 1000–1050 cm^{-1} and 1390–1420 cm^{-1} wave number ranges clearly distinguished different tissues of different plant samples based on total cell wall composition, cellulose and lignin content, respectively.

ATR-FTIR in combination with KBr-based standard can quantify cellulose and lignin content

ATR-FTIR can efficiently be used for quantitative analysis of liquid samples but the homogenization is the major constraint for the quantification of powdered samples. Most of the cell wall material usually does not dissolve in organic solvent. Therefore, in this study emphasis was made on quantifying cell wall composition in solid form using ATR-FTIR by mixing commercially available standards (cellulose and lignin) with KBr in different concentrations. Wavenumber number regions 1050–1060 cm^{-1} and 1390–1420 cm^{-1} were used to detect cellulose and lignin, respectively. An absorbance gradient of 0.10, 0.12, 0.14 and 0.175 was observed for 10%, 20%, 30% and 40% cellulose, respectively (Fig. 3a). Similarly, 0.026, 0.036 and

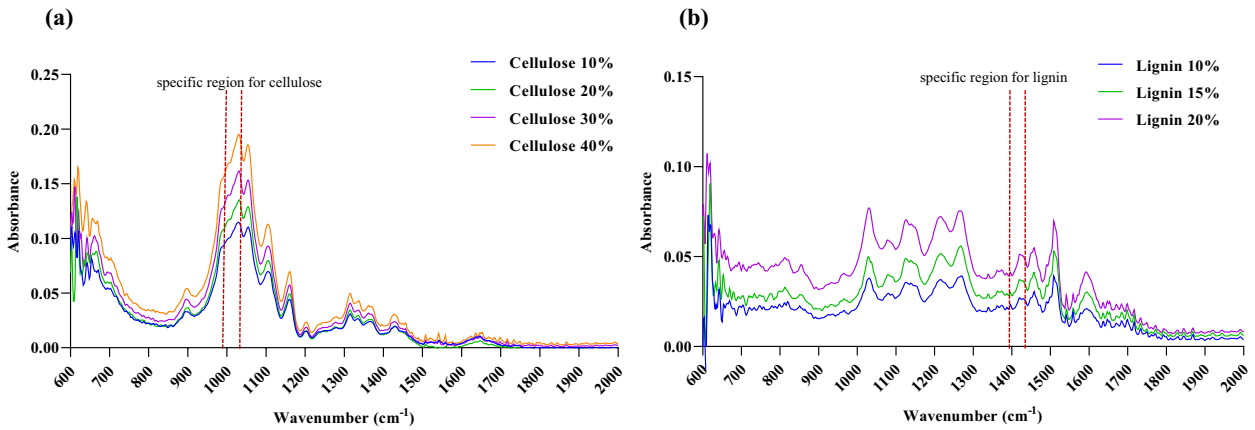

Fig. 3 Spectra represent the different concentrations of **a** cellulose and **b** lignin prepared using KBr. The dotted line represents selected region used for quantification. The spectral mean was calculated from two technical replicates

0.05 was observed for 10%, 15% and 20% lignin, respectively (Fig. 3b). The standard curve was prepared for both to quantify cellulose and lignin in different tissue types. Based on the standard curve, the stem of *Populus*, rice, Arabidopsis and mungbean contained 48.8%, 46.2%, 39.2% and 42.6% of cellulose, respectively. The leaves of *Populus*, rice, Arabidopsis and mungbean are composed of 34.0%, 52.4%, 12.1% and 18.1% of cellulose, respectively (Table 2). It was observed that rice leaf contains a high amount of cellulose, which was evident from multivariate analysis (Fig. 2b, Fig. S1b). The stem of *Populus,* rice, Arabidopsis and mungbean contained 16.3%, 23.4% 19.6% and 22.3% of lignin respectively. The leaf of *Populus,* rice, Arabidopsis and mungbean contained 20.8%, 23.4%, 24.1% and 34.7% of lignin, respectively. Generally, leaf tissue contains less lignin, and we hypothesized that lignin peaks probably interfere with other sugars or phenolics. To test this, AIR was treated with a high concentration of NaOH followed by digestion with cellulase to remove cellulose, and the remaining pellet mostly contained lignin, which was used for FT-IR analysis. However, the lignin content was higher in mungbean leaf followed by *Populus* stem, Arabidopsis stem and rice leaf; which was consistent with our previous observation. This data again confirmed that the selected region can be used to quantify the lignin content (Fig. 4).

FT-IR based quantification of lignin and cellulose validated by wet-chemistry methods

To check whether cell wall content calculated using FT-IR is correlating with wet-chemistry methods, the cellulose and lignin content were analysed by standard Updegraff and acetyl bromide soluble lignin method respectively. The result revealed that the cellulose content of Arabidopsis leaf, Arabidopsis stem, mungbean leaf, mungbean stem, *Populus* leaf, *Populus* stem, rice leaf and rice stem was 10.8%, 29.5%, 6.5%, 28.6%, 11.2%, 39.7%, 21.0% and 17.9% respectively (Fig. 5a). The total

Table 2 Cellulose and Lignin content of different plant samples measured using ATR-FTIR and wet-chemistry method

Species and tissue types	ATR-FTIR-based method		Wet-chemistry-based method		*p*-value for cellulose	*p*-value for lignin
	Cellulose (%) ± SD	Lignin (%) ± SD	Cellulose ± SD (%)	Lignin (%) ± SD		
Populus stem	48.9 ± 1.3	16.4 ± 0.4	39.7 ± 2.0	10.2 ± 0.4	0.062	0.008
Rice stem	46.2 ± 1.2	23.4 ± 2.8	17.9 ± 0.6	7.1 ± 0.8	0.002	0.082
Mungbean stem	42.6 ± 0.8	22.3 ± 0.6	28.7 ± 0.5	8.1 ± 0.6	0.003	0.0032
Arabidopsis stem	39.2 ± 1.7	19.6 ± 1.4	29.5 ± 2.5	7.5 ± 0.2	0.108	0.006
Populus leaf	34.0 ± 3.9	20.8 ± 0.6	11.2 ± 0.1	5.2 ± 0.3	0.028	0.002
Rice leaf	52.4 ± 4.9	23.4 ± 1.7	21.0 ± 0.9	7.5 ± 0.5	0.024	0.011
Mungbean leaf	18.1 ± 1.0	34.8 ± 1.1	6.5 ± 0.1	8.6 ± 0.3	0.0075	0.002
Arabidopsis leaf	12.1 ± 1.1	24.1 ± 1.2	10.8 ± 0.7	6.6 ± 0.05	0.48	0.012

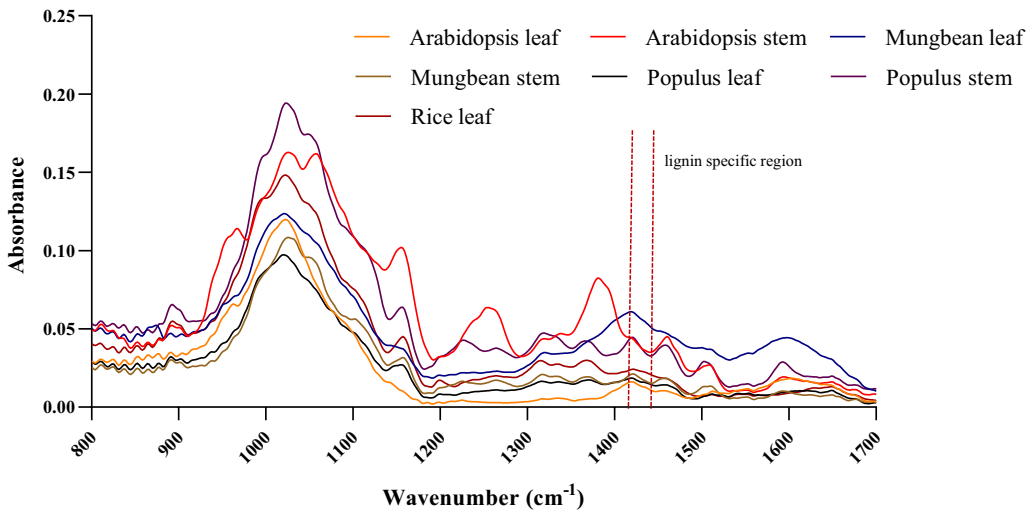

Fig. 4 Absorption spectral characteristics of samples after hemicellulose and cellulose removal which is enriched in lignin. Spectral mean was calculated from two different replicates

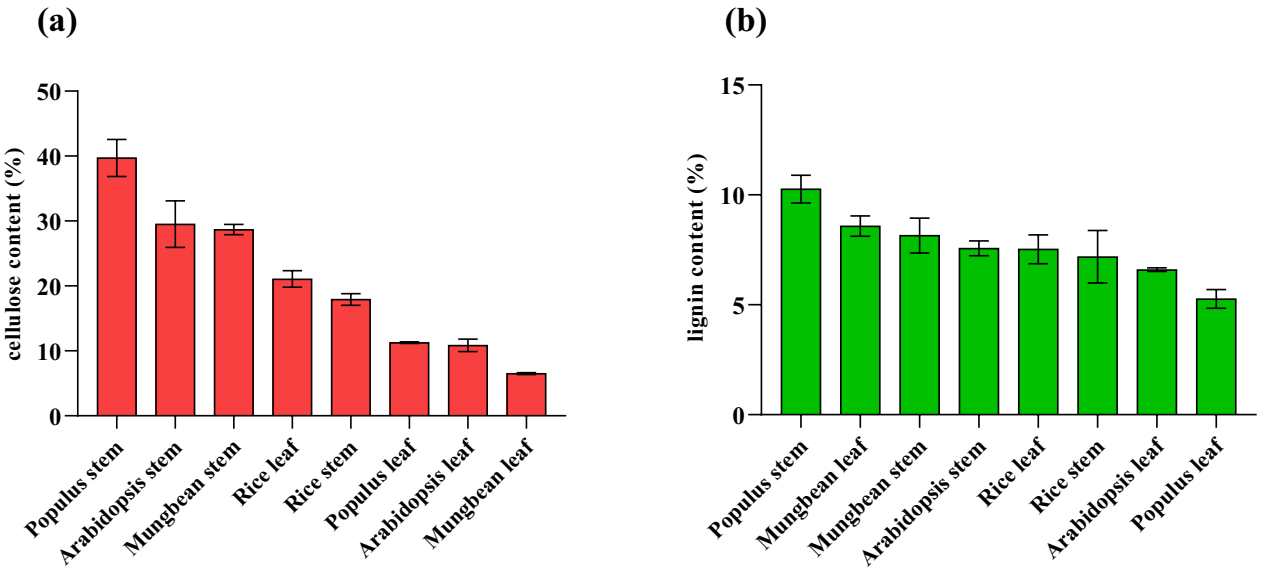

Fig. 5 Distribution of **a** cellulose and **b** lignin determined using Updegraf and acetyl bromide soluble lignin (ABSL) methods, respectively. Data represents mean ± SD with n = 2

sugar analysis was performed using phenol–sulfuric acid with slight modification and standardization [41]. This experiment validated the outcome of multivariate analysis and cellulose content among different tissues of different crop plants. The result suggested that Arabidopsis leaf, Arabidopsis stem, mungbean leaf, mungbean stem, *Populus* leaf, *Populus* stem, rice leaf, rice stem contain 8.8%, 53.3%, 18.9%, 52.4%, 26.2%, 61.4%, 44.6% and 43.9% total sugar (Fig. S3). It was evident that *Populus* stem contain the highest total sugar as compared to other species. However, rice leaf and stem contain comparatively equal amounts of total sugar, which correlated with cellulose content analysis. Whereas, the lignin content of Arabidopsis leaf, Arabidopsis stem, mung leaf, mung stem, *Populus* leaf, *Populus* stem, rice leaf and rice stem were found to be 6.6%, 7.5%, 8.58%, 8.1%, 5.2%, 10.2%, 7.5% and 7.1% respectively (Fig. 5b). Histochemical analysis revealed differential pattern of lignification within stem section of Arabidopsis, mungbean and rice (Fig S4; S5). This differentiation may be due to the variation in many lignified xylem cells or tissues rather than increased lignification of xylem cells or tissues. However, detailed analyses are needed to get insight into the intricate mechanism of the cellular lignification process among different plant species. The analysis using both methods revealed that stem cellulose content was higher as compared to leaf in all the plant sample, which was also validated using total sugar analysis. In the case of lignin, the wet-chemistry analysis revealed that the stem lignin content is higher as compared to leaf lignin. However, the FTIR analysis revealed that leaf lignin content is higher as compared to leaf lignin measured using the wet-chemistry method.

High throughput screening of cell wall composition of mungbean accessions revealed validation of wavenumber for cellulose and lignin

Our results suggested that ATR-FTIR can be used for quantification of cellulose and lignin. Therefore, we analyzed and validated the cell wall composition of different mungbean accessions. Though mungbean is an important legume, the large-scale qualitative and quantitative analysis of its cell wall composition was never performed earlier. Therefore, the main stem from field-grown mungbean accessions was collected and subjected to ATR-FTIR and wet-chemistry-based analysis of cell wall composition. The percentage of cellulose content determined by the ATR-FTIR-based method was 10–15% higher as compared to the percentage determined by the Updegraff method (Fig. 6a; Table S1).

Chemical analysis revealed that the total cellulose content variation ranges from 23.2% (KM 11–40) to 39.5% (ML 1451) with a mean value of 31.2%. The comparatively lower cellulose containing genotypes were KM 11–40 (23.2%), IPM 02–17 (23.4%), IC 282094 (23.6%), LGG 460 (24.4%), KM 2241 (25.7%), IPM 288 (25.9%), HUM 6 (26.7%), CHINA MUNG (27.3%), M 875 (27.8%) and M 880 (28.0%). The higher cellulose-containing genotypes are GANGA 1 (35.9%), M 565 (36.5%), KM 16–75 (36.8%), TM 9725 (37.1%), MH 934 (37.2%), PUSA 1331 (37.9%), IPM 409–4 (38.3%), PLM 167 (38.5%), EC

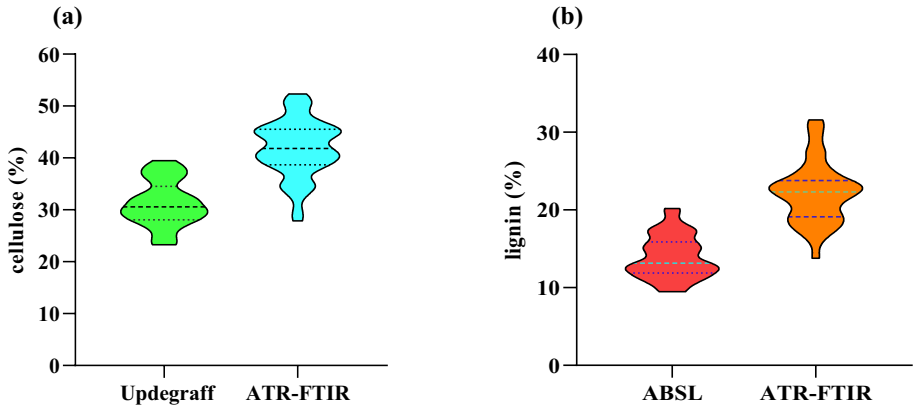

Fig. 6 Distribution of **a** cellulose and **b** lignin content using ATR-FTIR and wet-chemistry methods. Data represents the average from 48 mungbean accessions

550851 (38.6%) and ML 1451 (39.5%). The ATR-FTIR-based study revealed the cellulose content variation ranges from 27.9% (KM 11–40) to 52.3% (M 565) with a mean value of 41.8% (Fig. 6a). In the case of the ATR-FTIR-based spectroscopic approach, the comparatively lower cellulose-containing genotypes were KM 11–40 (27.9%), M 499 (29.7%), IC 282094 (32.6%), CHINA MUNG (33.7%), PLM 167 (34.5%), EC 3988891 (34.7%), M 1400 (35.0%), YM 2 (35.1%), EC 520026 (37.6%), PUSA 1441 (38.0%). The higher cellulose-containing genotypes were PUSA 1131 (45.7%), KM 16–58 (45.8%), M 1053 (46.8%), KM 16–75 (47.3%), MH 934 (47.4%), OLRM 4 (49.4%), ML 1451 (50.4%), EC 550851 (50.8%), TM 9725 (51.0%) and M 565 (52.3%) (Fig. 6a, Table S1). The cellulose content was lower in KM 11–40, IC 282094 and CHINA MUNG using wet-chemistry and ATR-FTIR method. We also found that M 565, KM 16–75, TM 9725, MH 934, EC 550851 and ML 1451 had higher cellulose content using both approaches.

In a separate set of 48 accessions, lignin content was determined using the ATR-FTIR-based and acetyl bromide soluble lignin (ABSL) measurement approach. The lignin content determined by the ATR-FTIR-based method was 5–10% higher as compared to the percentage determined by the ABSL method (Fig. 6b and Table S2). Chemical analysis revealed that the total lignin content variation ranges from 9.4% (EC 520029) to 20.2% (M 313) with a mean value of 13.9% (Fig. 6b). The lower lignin content genotypes were EC 520029 (9.4%), IC 282094 (9.4%), M 880 (9.5%), SML 668 (10.4%), MUSKAN (10.7%), KM 11–40 (10.9%), PUSA 1131 (11.0%), M 1053 (11.1%), PUSA VISHAL (11.3%) and M 1400 (11.4%). The higher lignin content genotypes were IPM 288 (16.8%), M 906 (16.9%), V 1153 (17.3%), KM 7–134 (17.3%), HUM 1 (17.9%), PUSA 0971 (17.6%), MH 96–1 (17.7%), IPM 02–19 (18.8%) M 1370 (19.9%) and M 313 (20.2%). The ATR-FTIR-based study revealed the lignin content variation ranges from 13.7% (M 875) to 31.6% (M 313) with a mean value of 22.2%. The lower lignin content genotypes using ATR-FTIR approach were M 875 (13.7%), PUSA 0971 (15.7%), EC 520029 (16.9%) M 1400 (17.2%), M 1032 (17.2%), IC 282094 (17.5%), PUSA 1441 (18.8%), PUSA VISHAL (18.2%), MH 96–1 (18.4%) and TM 96–25 (18.7%). The higher lignin content genotypes were HUM 1 (25.1%), PUSA 1342 (25.1%), M 831 (25.2%), TM 96–2 (26.7%), V 1153 (27.2%), IPM 02–19 (27.7%), IPM 02–17 (29.0%), KM 7–134 (30.0%), M 1370 (31.0%), M 313 (31.6%) (Table S2). The genotypes, EC 520029, IC 282094, PUSA VISHAL and M 1400 had the comparatively lower lignin content using both the ATR-FTIR and wet-chemistry-based methods. The genotypes V 1153, KM 7–134, HUM 1, IPM 02–19, M 1370 and M 313 contained comparatively higher lignin in both methods. The reason behind mis-correlation between FT-IR data with wet chemistry is because of overlapping peaks corresponding to different functional groups of cell wall components. Overall, this data revealed that ATR-FTIR-based quantification can be used for high throughput analysis of cellulose and lignin.

Discussion

The samples from diverse plant species were selected to cover the variability of cell wall composition for qualitative and quantitative estimation of its composition. In this study, two different approaches, ATR-FTIR and wet-chemical based method were used to determine cell wall composition of leaf and stem tissues from *Populus*, rice, mungbean and Arabidopsis. *Populus* is highly desirable as a feedstock for biofuels as compared to other woody crops. It grows fast and produces a significant amount of biomass within a short period. Moreover, the stem of *Populus* is a source of high cellulose (45–50%), hemicellulose

(20–25%) and lignin (25–30%) [61–63]. The higher cellulose content could be because of tension wood formation in *Populus* wood. The stem and leaf cellulose and lignin content of *Populus* have been measured in several studies [51, 56, 64–69]. The stem cellulose content was reported around 40–45% in several studies [51, 56, 66, 67] that is consistent with our measurement of around 40% stem cellulose. The leaf cellulose content of *Populus* was found to be around 10–12% [56, 64, 65] and similar content was observed in our study (Fig. 5). The stem lignin was varied from 10 to 15% in different studies [68, 69], which is in line with our determination of 10–12% stem lignin content. The biomass of mature rice cell walls is usually composed of 40%-50% cellulose, 20–25% hemicellulose and 20–25% lignin, and most rice residue (straw and husk) biomass is underutilized [60], which can be effectively used for bioenergy feedstock. In rice there are several studies determining cellulose content in leaf and stem [70–72]. Stem cellulose content in rice is highly dynamic depending on the developmental stages and tissue types. Zhang et al. (2017) reported around 20% stem cellulose at the heading stage, correlating with our study that reports 18–20% stem cellulose content. Leaf cellulose content of rice has also been determined in several studies [71, 72]. Luan et al. (2022) reported that rice leaf contains 21–23% cellulose, correlating our determination of 21–22% leaf cellulose content (Fig. 5). The lignin content of rice has also been determined in different studies [73–75]. Two different studies were performed by Jung et al. 2022 and Bang et al. 2019 reported 8–10% of lignin in leaf and stem, which was consistent with our analysis i.e., 7–8% in both tissues. Arabidopsis is a plant model system wherein plant cell wall is extensively studied. Arabidopsis stem cell wall biomass is reported to be composed of 40–45% cellulose, 15–20% hemicellulose and 10–15% lignin [64, 75]. In Arabidopsis, several studies were performed to analyse cellulose content in stem and leaf tissue [23, 76–78]. Takahashi et al. [23] reported around 35–37% of stem cellulose, which is in line with our study that suggested around 30–32% stem cellulose (Fig. 5a). In Arabidopsis leaf tissue, cellulose composition was reported around 10–14%. In our study, around 10–12% of cellulose has been determined in Arabidopsis leaf (Fig. 5). In Arabidopsis, the lignin content was determined in several studies as around 8–10% by the ABSL method that was in line with our report of 8–9% stem lignin [79–82]. Overall, wet chemistry data revealed similar cell wall composition in species and tissue types with available literature that can be compared with FT-IR quantification for further validation.

Several studies revealed that the cell wall composition is dynamic across different plant species [2]. Moreover, most of these cell wall components are water-insoluble. Thus, it is challenging to quantify the cell wall composition using ATR-FTIR in powder form. Therefore, in this study, efforts have been put forward for quantitative and qualitative analysis of plant cell wall composition in powder form which is compared with wet chemistry data. Gorzsás et al. [21] and Canteri et al. [43] reported several regions for cell wall composition, including cellulose and lignin in different plant species. However, in the present study, regions for cellulose and lignin were identified by comparing monocot (rice), dicot (Arabidopsis and mungbean) and eudicot (*Populus*) species. Specific regions were identified for analysis of total cell wall composition (800–2000 cm^{-1}), cellulose (1000–1050 cm^{-1}) and lignin (1390–1420 cm^{-1}). Multivariate analysis revealed a clear grouping of leaf and stem samples of monocot, dicot and eudicot species in these regions suggesting our method can capture variation in cell wall composition (Fig. 2, Fig. S1, S2). This data concluded that the selected wavenumber region can be used to compare cellulose and lignin content with different spectral characteristics. To date, mostly the cell wall can be quantified using canonical wet chemistry-based method. These methods are time-consuming, costly and non-high throughput. Also, the quantification of lignin and cellulose are performed with separate methods. Using our proposed method, they were quantified in a single run with less amount of sample.

Also, quantitative analysis using ATR-FTIR indicated that stem cellulose content of all the plant species is higher as compared to leaf. However, it has been observed that leaf lignin content is slightly higher as compared to stem lignin content. In general, leaf tissue contains less lignin, and we hypothesized that lignin-specific region probably interfere with other sugars or phenolics. Therefore, extraction of lignin-rich fraction was performed from AIR to analyse using FT-IR (Fig. 4). We found that the lignin content was higher in mungbean leaf followed by *Populus* stem, Arabidopsis stem and rice leaf; validating that the selected region can be used to quantify the lignin content (Fig. 4). Further, the result of FTIR-based quantification method was validated by using the canonical wet chemistry method. The wet-chemistry-based approach revealed that rice leaf, stem and mung leaf contain comparatively less cellulose than ATR-FTIR data, probably because of overlapping peaks from other matrix polysaccharide components [21].

Moreover, the large-scale quantitative analysis of cell wall composition in different accessions of mungbean was performed using identified specific region for cellulose and lignin. The region for cellulose (1000–1050 cm^{-1}) and lignin (1390–1420 cm^{-1}) were found specific for monocot, dicot and eudicot species.

Therefore, these regions were used to quantify cell wall composition in mungbean. The percentage of cellulose by ATR-FTIR-based method was 10–15% higher as compared to the percentage determined by the Updegraff method (Fig. 6). This variation can be explained by the presence of non-crystalline cellulose or from other hemicellulosic polysaccharide that can be measured using the ATR-FTIR-based method but not by the Updegraff method [9, 83]. In general, plant cell wall consists of around 10–20% amorphous cellulose depending on plant and tissue types [84, 85]. During cell wall material preparation, amorphous cellulose was removed, and the remaining pellet was used for Updegraff analysis. This non-crystalline form of cellulose can only be detected using a spectroscopic approach but not using the Updegraff method since it is removed during the extraction process [86]. The lignin content determined by the ATR-FTIR-based method was found to be 5–10% higher as compared to the percentage determined by the ABSL method. In our study, lignin has been detected within 1390–1420 cm^{-1} wavenumber for C-H deformation of aromatic skeletal vibrations. Lignin monomers are synthesized through the phenylpropanoid pathway [87]. Therefore, it is possible that within this range of wavenumber, some derivative compounds having C-H deformation of aromatic skeletal vibrations can be overlapping. The reason for miscorrelation between the two methods could be the same wavenumber can represent peaks for different components. The ideal way would be to perform sequential extraction of varying cell wall components and analyse their composition using FT-IR and wet chemistry methods. Overall, the combined effort of ATR-FTIR-based and chemical methods led to the determination of stem cellulose and lignin content of several mungbean accessions. To the best of our knowledge, there are no reports on the characterization of polysaccharides in mungbean. Few reports are based on the isolation of soluble polysaccharides, characterization of mono or oligosaccharides and their role in inducing the immunomodulatory properties [88]. Mungbean stem and leaf tissues are repertoire of complex polysaccharides, but their characterization was not done before. In our study, we found that the average stem cellulose content is around 32% (Updegraff method) and 42% (ATR-FTIR) in mungbean. The stem lignin content is found to be around 14% (Updegraff method) and 22% (ATR-FTIR) (Fig. 6). This approach also leads to relatively discriminating stem cellulose and lignin content among different mungbean accessions. This data suggested that ATR-FTIR can be used for the relative quantification of lignin and cellulose in mungbean and different crop species.

Conclusion

ATR-FTIR is conveniently applicable with simple chemometric and multivariate analysis to predict the cell wall composition in different plant species. In this study, a high-throughput, non-destructive, powerful approach has been developed for qualitative and quantitative analysis of solid cell wall material which is not dissolved in organic solvent. This method has been used to determine the cellulose and lignin content among different mungbean accessions. Further, the wet-chemistry analyses have been performed to validate the outcome of the ATR-FTIR-based method. This approach can be used for large-scale chemotyping of cell wall composition among different plant species. Thus, it could reduce cost, time and labour in breeding programs. The method and strategy presented in this study can accelerate large-scale cell wall compositional analysis among thousands of accessions. Therefore, it has immense potential in molecular breeding, such as QTL-mapping, genome or candidate gene-based association mapping and thus, could enhance the pace of genomics-assisted breeding.

Supplementary Information

The online version contains supplementary material available at https://doi.org/10.1186/s13007-024-01260-w.

Additional file 1: Table S1. Determination of cellulose content among 48 accessions of mungbean, using Updegraff and ATR-FTIR-based method.

Additional file 2: Table S2. Determination of lignin content among 48 accessions of mungbean, using ABSL and ATR-FTIR-based method.

Additional file 3: Figure S1. Principal component analysis of absorption spectra within. **a** 800–2000 cm^{-1}; **b** 1000–1100 cm^{-1}; **c** 1390–1420 cm^{-1} wavenumber for total sugar, cellulose, and lignin respectively in ATR-FTIR. Figure S2. K-mer analysis of absorption spectra within. **a** 800–2000 cm^{-1}; **b** 1000–1100 cm^{-1}; and **c** 1390–1420 cm^{-1} âwavenumber for total sugar, cellulose, and lignin respectively in ATR-FTIR. Figure S3. Total cell wall sugar analysis by phenol–sulphuric acid method. Data represents mean ± SD with n = 2. Figure S4. Phloroglucinol-HCl staining of stem section with 10× and 40× magnification for Arabidopsis; Mungbeanand Rice. Figure S5. Toluidine blue O staining of stem section with 10× and 40× magnification for Arabidopsis; Mungbeanand Rice.

Acknowledgements

We would like to thank RCB-Central Instrumentation facility and in-charge Vijay Jha for his technical support.

Author contributions

SD and PM-AP designed and conceptualized the research. SD, VB and AG performed all the experimental and data analysis. BPD performed total sugar analysis experiment. SD and PM-AP wrote the manuscript. HKD and GPM provided mungbean accession and suggestions during manuscript preparation. All authors have read and agreed to publish the manuscript.

Funding

This work is supported by DBT-MKB fellowship (102/IFD/SAN/2570/2021-22).

Availability of data and materials
No datasets were generated or analysed during the current study.

Declarations

Ethics approval and consent to participate
No specific permit was required for the samples analyzed in this study. The authors comply with relevant institutional, national, and international guidelines and legislation for plant studies.

Consent for publication
Not applicable.

Competing interests
The authors declares no competing interests.

Author details
[1]Laboratory of Plant Cell Wall Biology, Regional Centre for Biotechnology, NCR Biotech Science, Cluster 3rd Milestone, Faridabad-Gurgaon Expressway, Faridabad 121001, Haryana, India. [2]Division of Genetics, Indian Agricultural Research Institute, New Delhi 110012, India.

Received: 10 April 2024 Accepted: 19 August 2024
Published online: 02 September 2024

References

1. Somerville C, Bauer S, Brininstool G, Facette M, Hamann T, Milne J, et al. Toward a systems approach to understanding plant cell walls. Science. 1979;2004(306):2206–11.
2. Cosgrove DJ. Growth of the plant cell wall. Nat Rev Mol Cell Biol. 2005;6:850–61.
3. Houston K, Tucker MR, Chowdhury J, Shirley N, Little A. The plant cell wall: a complex and dynamic structure as revealed by the responses of genes under stress conditions. Front Plant Sci. 2016;7:984.
4. Hoffmann N, King S, Samuels AL, McFarlane HE. Subcellular coordination of plant cell wall synthesis. Dev Cell. 2021;56:933–48.
5. Ishida K, Noutoshi Y. The function of the plant cell wall in plant–microbe interactions. Plant Physiol Biochem. 2022;192:273–84.
6. Farrokhi N, Burton RA, Brownfield L, Hrmova M, Wilson SM, Bacic A, et al. Plant cell wall biosynthesis: genetic, biochemical and functional genomics approaches to the identification of key genes. Plant Biotechnol J. 2006;4:145–67.
7. Caffall KH, Mohnen D. The structure, function, and biosynthesis of plant cell wall pectic polysaccharides. Carbohydr Res. 2009;344:1879–900.
8. Barnes W, Anderson C. Acetyl bromide soluble lignin (ABSL) assay for total lignin quantification from plant biomass. Bio Protoc. 2017;7: e2149.
9. Dampanaboina L, Yuan N, Mendu V. Estimation of crystalline cellulose content of plant biomass using the Updegraff method. J Vis Exp. 2021. https://doi.org/10.3791/62031.
10. Pettolino FA, Walsh C, Fincher GB, Bacic A. Determining the polysaccharide composition of plant cell walls. Nat Protoc. 2012;7:1590–607.
11. Ding S-Y, Xu Q, Crowley M, Zeng Y, Nimlos M, Lamed R, et al. A biophysical perspective on the cellulosome: new opportunities for biomass conversion. Curr Opin Biotechnol. 2008;19:218–27.
12. Lupoi JS, Smith-Moritz A, Singh S, McQualter R, Scheller HV, Simmons BA, et al. Localization of polyhydroxybutyrate in sugarcane using Fourier-transform infrared microspectroscopy and multivariate imaging. Biotechnol Biofuels. 2015;8:98.
13. Galletti GC, Bocchini P. Pyrolysis/gas chromatography/mass spectrometry of lignocellulose. Rapid Commun Mass Spectrom. 1995;9:815–26.
14. Gierlinger N. New insights into plant cell walls by vibrational microspectroscopy. Appl Spectrosc Rev. 2018;53:517–51.
15. Holden CA, Bailey JP, Taylor JE, Martin F, Beckett P, McAinsh M. Know your enemy: application of ATR-FTIR spectroscopy to invasive species control. PLoS ONE. 2022;17: e0261742.
16. Fellah A, Anjukandi P, Waterland MR, Williams MAK. Determining the degree of methylesterification of pectin by ATR/FT-IR: Methodology optimisation and comparison with theoretical calculations. Carbohydr Polym. 2009;78:847–53.
17. López-Sánchez M, Ayora-Cañada MJ, Molina-Díaz A, Siam M, Huber W, Quintás G, et al. Determination of enzyme activity inhibition by FTIR spectroscopy on the example of fructose bisphosphatase. Anal Bioanal Chem. 2009;394:2137–44.
18. Szymanska-Chargot M, Zdunek A. Use of FT-IR spectra and PCA to the bulk characterization of cell wall residues of fruits and vegetables along a fraction process. Food Biophys. 2013;8:29–42.
19. Fahey LM, Nieuwoudt MK, Harris PJ. Predicting the cell-wall compositions of *Pinus radiata* (radiata pine) wood using ATR and transmission FTIR spectroscopies. Cellulose. 2017;24:5275–93.
20. Lee LC, Liong C-Y, Jemain AA. A contemporary review on data preprocessing (DP) practice strategy in ATR-FTIR spectrum. Chemom Intell Lab Syst. 2017;163:64–75.
21. Gorzsás A, Stenlund H, Persson P, Trygg J, Sundberg B. Cell-specific chemotyping and multivariate imaging by combined FT-IR microspectroscopy and orthogonal projections to latent structures (OPLS) analysis reveals the chemical landscape of secondary xylem. Plant J. 2011;66:903–14.
22. Jasinski S, Lécureuil A, Durandet M, Bernard-Moulin P, Guerche P. Arabidopsis seed content QTL mapping using high-throughput phenotyping: the assets of near infrared spectroscopy. Front Plant Sci. 2016;7:1682.
23. Takahashi D, Gorka M, Erban A, Graf A, Kopka J, Zuther E, et al. Both cold and sub-zero acclimation induce cell wall modification and changes in the extracellular proteome in *Arabidopsis thaliana*. Sci Rep. 2019;9:2289.
24. Fairbrother TE, Brink GE. Determination of cell wall carbohydrates in forages by near infrared reflectance spectroscopy. Anim Feed Sci Technol. 1990;28:293–302.
25. Molano ML, Cortés ML, Ávila P, Martens SD, Muñoz LS. Ecuaciones de calibración en espectroscopía de reflectancia en el infrarrojo cercano (NIRS) para predicción de parámetros nutritivos en forrajes tropicales. Trop Grassl Forrajes Trop. 2016;4:139.
26. Baldy A, Jacquemot M-P, Griveau Y, Bauland C, Reymond M, Mechin V. Energy values of registered corn forage hybrids in france over the last 20 years rose in a context of maintained yield increase. Am J Plant Sci. 2017;08:1449–61.
27. Li K, Wang H, Hu X, Ma F, Wu Y, Wang Q, et al. Genetic and quantitative trait locus analysis of cell wall components and forage digestibility in the Zheng58 × HD568 maize RIL population at anthesis stage. Front Plant Sci. 2017;8:1472.
28. Deng G, Nagy C, Yu P. Combined molecular spectroscopic techniques (SR-FTIR, XRF, ATR-FTIR) to study physiochemical and nutrient profiles of *Avena sativa* grain and nutrition and structure interactive association properties. Crit Rev Food Sci Nutr. 2023;63:7225–37.
29. Huang J, Li Y, Wang Y, Chen Y, Liu M, Wang Y, et al. A precise and consistent assay for major wall polymer features that distinctively determine biomass saccharification in transgenic rice by near-infrared spectroscopy. Biotechnol Biofuels. 2017;10:294.
30. Pushpa SR, Sukumaran RK, Savithri S. Rapid quantification of lignocellulose composition in rice straw varieties using artificial neural networks and FTIR spectroscopic data. Biomass Convers Biorefin. 2023. https://doi.org/10.1007/s13399-023-05032-9.
31. Gebreselassie MN, Ader K, Boizot N, Millier F, Charpentier J-P, Alves A, et al. Near-infrared spectroscopy enables the genetic analysis of chemical properties in a large set of wood samples from *Populus nigra* (L.) natural populations. Ind Crops Prod. 2017;107:159–71.
32. Wittner N, Slezsák J, Broos W, Geerts J, Gergely S, Vlaeminck SE, et al. Rapid lignin quantification for fungal wood pretreatment by ATR-FTIR spectroscopy. Spectrochim Acta A Mol Biomol Spectrosc. 2023;285: 121912.
33. Smith BC. Proper use of spectral processing in fundamentals of Fourier transform infrared spectroscopy. 2nd ed. New York: CRC Press; 2011.
34. Swinehart DF. The Beer-Lambert law. J Chem Educ. 1962;39:333.
35. Merriman S, Chandra D, Borowczak M, Dhinojwala A, Benko D. Simultaneous determination of additive concentration in rubber using ATR-FTIR spectroscopy. Spectrochim Acta A Mol Biomol Spectrosc. 2022;281: 121614.
36. Dai F, Zhuang Q, Huang G, Deng H, Zhang X. Infrared spectrum characteristics and quantification of OH groups in coal. ACS Omega. 2023;8:17064–76.

37. Pawar PM, Ratke C, Balasubramanian VK, Chong S, Gandla ML, Adriasola M, et al. Downregulation of RWA genes in hybrid aspen affects xylan acetylation and wood saccharification. New Phytol. 2017;214:1491–505.
38. Leyva A, Quintana A, Sánchez M, Rodríguez EN, Cremata J, Sánchez JC. Rapid and sensitive anthrone–sulfuric acid assay in microplate format to quantify carbohydrate in biopharmaceutical products: method development and validation. Biologicals. 2008;36:134–41.
39. Foster CE, Martin TM, Pauly M. Comprehensive compositional analysis of plant cell walls (lignocellulosic biomass) part i: lignin. J Vis Exp. 2010. https://doi.org/10.3791/1745.
40. Pradhan Mitra P, Loqué D. Histochemical staining of *Arabidopsis thaliana* secondary cell wall elements. J Vis Exp. 2014. https://doi.org/10.3791/51381.
41. Pattathil S, Avci U, Miller JS, Hahn MG. Immunological approaches to plant cell wall and biomass characterization: glycome profiling. In: Himmel ME, editor. Biomass conversion. Totowa: Humana Press; 2012. p. 61–72.
42. Türker-Kaya S, Huck C. A review of mid-infrared and near-infrared imaging: principles, concepts and applications in plant tissue analysis. Molecules. 2017;22:168.
43. Canteri MHG, Renard CMGC, Le Bourvellec C, Bureau S. ATR-FTIR spectroscopy to determine cell wall composition: application on a large diversity of fruits and vegetables. Carbohydr Polym. 2019;212:186–96.
44. Mouille G, Robin S, Lecomte M, Pagant S, Höfte H. Classification and identification of *Arabidopsis* cell wall mutants using Fourier-Transform InfraRed (FT-IR) microspectroscopy. Plant J. 2003;35:393–404.
45. Alonso-Simón A, García-Angulo P, Mélida H, Encina A, Álvarez JM, Acebes JL. The use of FTIR spectroscopy to monitor modifications in plant cell wall architecture caused by cellulose biosynthesis inhibitors. Plant Sign Behav. 2011;6:1104–10.
46. Kačuráková M, Smith AC, Gidley MJ, Wilson RH. Molecular interactions in bacterial cellulose composites studied by 1D FT-IR and dynamic 2D FT-IR spectroscopy. Carbohydr Res. 2002;337:1145–53.
47. Sun R. Fractional isolation, physico-chemical characterization and homogeneous esterification of hemicelluloses from fast-growing poplar wood. Carbohydr Polym. 2001;44:29–39.
48. Labbi N, Rials TG, Kelley SS, Cheng Z-M, Kim J-Y, Li Y. FT-IR imaging and pyrolysis-molecular beam mass spectrometry: new tools to investigate wood tissues. Wood Sci Technol. 2005;39:61–76.
49. Faix O, Bremer J, Schmidt O, Tatjana SJ. Monitoring of chemical changes in white-rot degraded beech wood by pyrolysis—gas chromatography and Fourier-transform infrared spectroscopy. J Anal Appl Pyrolysis. 1991;21:147–62.
50. Sun R, Sun XF. Structural and thermal characterization of acetylated rice, wheat, rye, and barley straws and poplar wood fibre. Ind Crops Prod. 2002;16:225–35.
51. Yu P. Applications of hierarchical cluster analysis (CLA) and principal component analysis (PCA) in feed structure and feed molecular chemistry research, using synchrotron-based Fourier transform infrared (FTIR) microspectroscopy. J Agric Food Chem. 2005;53:7115–27.
52. Gou J-Y, Park S, Yu X-H, Miller LM, Liu C-J. Compositional characterization and imaging of "wall-bound" acylesters of *Populus trichocarpa* reveal differential accumulation of acyl molecules in normal and reactive woods. Planta. 2008;229:15–24.
53. Boeriu CG, Bravo D, Gosselink RJA, van Dam JEG. Characterisation of structure-dependent functional properties of lignin with infrared spectroscopy. Ind Crops Prod. 2004;20:205–18.
54. Naumann A, Polle A. FTIR imaging as a new tool for cell wall analysis of wood. N Z J For Sci. 2006;36:54–9.
55. Sun R. Fractional isolation and physico-chemical characterization of alkali-soluble lignins from fast-growing poplar wood. Polymer (Guildf). 2000;41:8409–17.
56. Huang C, Han L, Liu X, Ma L. The rapid estimation of cellulose, hemicellulose, and lignin contents in rice straw by near infrared spectroscopy. Energy Sourc Part A Recover Utilization Environ Eff. 2010;33:114–20.
57. Pawar PM-A, Schnürer A, Mellerowicz EJ, Rönnberg-Wästljung AC. QTL mapping of wood FT-IR chemotypes shows promise for improving biofuel potential in short rotation coppice willow (Salix spp.). Bioenergy Res. 2018;11:351–63.
58. Szymańska E, Saccenti E, Smilde AK, Westerhuis JA. Double-check: validation of diagnostic statistics for PLS-DA models in metabolomics studies. Metabolomics. 2012;8:3–16.
59. Chen C, Chen Z, Chen J, Huang J, Li H, Sun S, et al. Profiling of chemical and structural composition of lignocellulosic biomasses in tetraploid rice straw. Polymers (Basel). 2020;12:340.
60. Chen C, Qu B, Wang W, Wang W, Ji G, Li A. Rice husk and rice straw torrefaction: properties and pyrolysis kinetics of raw and torrefied biomass. Environ Technol Innov. 2021;24: 101872.
61. Davis JM. Genetic improvement of poplar (Populus spp.) as a bioenergy crop. In: Vermerris W, editor. Genetic improvement of bioenergy crops. New York: Springer; 2008. p. 397–419.
62. Sannigrahi P, Ragauskas AJ, Tuskan GA. Poplar as a feedstock for biofuels: a review of compositional characteristics. Biofuels Bioprod Biorefin. 2010;4:209–26.
63. Littlewood J, Guo M, Boerjan W, Murphy RJ. Bioethanol from poplar: a commercially viable alternative to fossil fuel in the European Union. Biotechnol Biofuels. 2014;7:113.
64. Ohmiya Y, Takeda T, Nakamura S, Sakai F, Hayashi T. Purification and properties of wall-bound endo-1, 4-beta-glucanase from suspension-cultured poplar cells. Plant Cell Physiol. 1995;36:607–14.
65. Xu H, Liang M, Xu L, Li H, Zhang X, Kang J, et al. Cloning and functional characterization of two abiotic stress-responsive Jerusalem artichoke (*Helianthus tuberosus*) fructan 1-exohydrolases (1-FEHs). Plant Mol Biol. 2015;87:81–98.
66. Wegrzyn JL, Eckert AJ, Choi M, Lee JM, Stanton BJ, Sykes R, et al. Association genetics of traits controlling lignin and cellulose biosynthesis in black cottonwood (*Populus trichocarpa*, Salicaceae) secondary xylem. New Phytol. 2010;188:515–32.
67. Park YW, Baba K, Furuta Y, Iida I, Sameshima K, Arai M, et al. Enhancement of growth and cellulose accumulation by overexpression of xyloglucanase in poplar. FEBS Lett. 2004;564:183–7.
68. Wildhagen H, Paul S, Allwright M, Smith HK, Malinowska M, Schnabel SK, et al. Genes and gene clusters related to genotype and drought-induced variation in saccharification potential, lignin content and wood anatomical traits in *Populus nigra*. Tree Physiol. 2018;38:320–39.
69. Rubinelli PM, Chuck G, Li X, Meilan R. Constitutive expression of the Corngrass1 microRNA in poplar affects plant architecture and stem lignin content and composition. Biomass Bioenergy. 2013;54:312–21.
70. Chen Y, Dan Z, Gao F, Chen P, Fan F, Li S. *Rice GROWTH-REGULATING FACTOR7* modulates plant architecture through regulating ga and indole-3-acetic acid metabolism. Plant Physiol. 2020;184:393–406.
71. Zhang J, Li G, Huang Q, Liu Z, Ding C, Tang S, et al. Effects of culm carbohydrate partitioning on basal stem strength in a high-yielding rice population. Crop J. 2017;5:478–87.
72. Luan W, Liu Y, Zhang F, Song Y, Wang Z, Peng Y, et al. *OsCD1* encodes a putative member of the cellulose synthase-like D sub-family and is essential for rice plant architecture and growth. Plant Biotechnol J. 2011;9:513–24.
73. Xie J, Kong X, Chen J, Hu B, Wen P, Zhuang J, et al. Mapping of quantitative trait loci for fiber and lignin contents from an interspecific cross Oryza sativa × Oryza rufipogon. J Zhejiang Univ Sci B. 2011;12:518–26.
74. Taylor LE, Dai Z, Decker SR, Brunecky R, Adney WS, Ding S-Y, et al. Heterologous expression of glycosyl hydrolases in planta: a new departure for biofuels. Trends Biotechnol. 2008;26:413–24.
75. Bang SW, Lee D, Jung H, Chung PJ, Kim YS, Do CY, et al. Overexpression of OsTF1L, a rice HD-Zip transcription factor, promotes lignin biosynthesis and stomatal closure that improves drought tolerance. Plant Biotechnol J. 2019;17:118–31.
76. Wang W, Viljamaa S, Hodek O, Moritz T, Niittylä T. Sucrose synthase activity is not required for cellulose biosynthesis in Arabidopsis. Plant J. 2022;110:1493–7.
77. Zablackis E, Huang J, Muller B, Darvill AG, Albersheim P. Characterization of the cell-wall polysaccharides of *Arabidopsis thaliana* leaves. Plant Physiol. 1995;107:1129–38.
78. Rui Y, Anderson CT. Functional analysis of cellulose and xyloglucan in the walls of stomatal guard cells of Arabidopsis. Plant Physiol. 2016;170:1398–419.
79. Moneo-Sánchez M, Vaquero-Rodríguez A, Hernández-Nistal J, Albornos L, Knox P, Dopico B, et al. Pectic galactan affects cell wall architecture during secondary cell wall deposition. Planta. 2020;251:100.

80. Capron A, Chang XF, Hall H, Ellis B, Beatson RP, Berleth T. Identification of quantitative trait loci controlling fibre length and lignin content in *Arabidopsis thaliana* stems. J Exp Bot. 2013;64:185–97.
81. Sibout R, Eudes A, Mouille G, Pollet B, Lapierre C, Jouanin L, et al. *CINNAMYL ALCOHOL DEHYDROGENASE-C* and *-D* are the primary genes involved in lignin biosynthesis in the floral stem of Arabidopsis. Plant Cell. 2005;17:2059–76.
82. Shigeto J, Itoh Y, Hirao S, Ohira K, Fujita K, Tsutsumi Y. Simultaneously disrupting AtPrx2, AtPrx25 and AtPrx71 alters lignin content and structure in Arabidopsis stem. J Integr Plant Biol. 2015;57:349–56.
83. Mense AL, Zhang C, Zhao J, Liu Q, Shi Y-C. Physical aspects of the biopolymer matrix in wheat bran and its dissected layers. J Cereal Sci. 2020;95:103002.
84. Marga F, Grandbois M, Cosgrove DJ, Baskin TI. Cell wall extension results in the coordinate separation of parallel microfibrils: evidence from scanning electron microscopy and atomic force microscopy. Plant J. 2005;43:181–90.
85. Voiniciuc C, Pauly M, Usadel B. Monitoring polysaccharide dynamics in the plant cell wall. Plant Physiol. 2018;176:2590–600.
86. Updegraff DM. Semimicro determination of cellulose inbiological materials. Anal Biochem. 1969;32:420–4.
87. Yao T, Feng K, Xie M, Barros J, Tschaplinski TJ, Tuskan GA, et al. Phylogenetic occurrence of the phenylpropanoid pathway and lignin biosynthesis in plants. Front Plant Sci. 2021;12:704697.
88. Hou D, Yousaf L, Xue Y, Hu J, Wu J, Hu X, et al. Mung bean (*Vigna radiata* L.): bioactive polyphenols, polysaccharides, peptides, and health benefits. Nutrients. 2019;11:1238.
89. Wilson RH, Smith AC, Kačuráková M, Saunders PK, Wellner N, Waldron KW. The mechanical properties and molecular dynamics of plant cell wall polysaccharides studied by Fourier-transform infrared spectroscopy. Plant Physiol. 2000;124:397–406.
90. Müller G, Polle A. Imaging of lignin and cellulose in hardwood using Fourier transform infrared microscopy—comparison of two methods. N Z J For Sci. 2009;39:225–31.
91. Naumann A, Navarro-González M, Peddireddi S, Kües U, Polle A. Fourier transform infrared microscopy and imaging: detection of fungi in wood. Fungal Genet Biol. 2005;42:829–35.
92. Hergert HL. Infrared spectra of lignin and related compounds. II. Conifer lignin and model compounds[1,2]. J Org Chem. 1960;25:405–13.

Publisher's Note